ISSN 1027-4510, Journal of Surface Investigation: X-ray, Synchrotron and Neutron Techniques, 2023, Vol. 17, No. 5, pp. 1143–1147. © Pleiades Publishing, Ltd., 2023.

Magnetron Deposition of Oxide Films in the Metallic Mode Enhanced by Radio-Frequency Inductively Coupled Plasma Source

D. V. Sidelev[a], * and E. D. Voronina[a]

[a] *Tomsk Polytechnic University, Tomsk, 634050 Russia*

**e-mail: sidelevdv@tpu.ru*

Received February 25, 2023; revised April 17, 2023; accepted April 17, 2023

Abstract—Magnetron sputtering of an yttrium target in a reactive atmosphere of $Ar + O_2$ enhanced by a radio-frequency inductively coupled plasma source was studied. Four different schemes for yttrium target sputtering were examined to define the possibility to use the metallic deposition mode for a coating consisting of the yttrium oxide phase. The effective pumping speeds were calculated for all experimental schemes. The increase in the effective pumping speed from 0.24 to ~0.87 m^3/s when using dual magnetron sputtering of Y and Cu targets was shown to result in the shift of the hysteresis loop towards higher O_2 flow rates. This leads to the use of both transition and metallic modes of Y target sputtering in the $Ar + O_2$ atmosphere. The oxide coating was deposited by dual magnetron sputtering of yttrium and copper targets in the metallic mode, enhanced by a radio-frequency inductively coupled plasma source. The coating consisted of Cu_2O and Y_2O_3 phases. The calculation of Cu and Y sputtering yields was done to confirm the metallic mode of coating deposition.

Keywords: reactive deposition, magnetron sputtering, oxide, coating deposition, thin films, metallic mode, radio-frequency inductively coupled plasma (RF-ICP), deposition rate, yttrium oxide, plasma assistance

DOI: 10.1134/S1027451023050166

INTRODUCTION

Yttrium oxide Y_2O_3 is a preferred candidate for protective coatings of high-temperature crucibles for melting metals and for optical waveguides [1–4]. It is possible to obtain Y_2O_3 coatings using reactive magnetron sputtering [5], based on collisional sputtering of an yttrium target by plasma ions and condensation of yttrium and oxygen atoms on the substrate. However, the presence of oxygen in a vacuum chamber can lead to instability of coating deposition, which is usually described by the hysteresis effect when a metal target is sputtered in a reactive atmosphere [6]. The hysteresis curve shows the state of the sputtered target at various flow rates of reactive gas. This can be represented by the dependence of the sputtering process parameters (discharge voltage, current, and oxygen partial pressure) on the flow rate of reactive gas. Usually, three modes of target sputtering are distinguished on the hysteresis curve: metallic, transition, and reactive. At a low flow rate of the reactive gas, the target is sputtered at a high rate, but the coating mainly consists of metal or substoichiometric phases. The reactive mode is characterized by the lowest deposition rate due to a decrease in the sputtering coefficient of the target material when a thin compound layer is formed on the target surface. The sputtering yields of the yttrium target in the metallic and reactive modes are 0.6 and 0.015 atom/ion, respectively [7]. The transition mode is between the metallic and reactive modes. Therefore, the metallic mode may be more preferable for coating deposition, since the deposition rate is maximal. However, it is also important to obtain the stoichiometry of the oxide coating, which can be difficult in the case of the metallic mode.

One of the approaches to the deposition of oxide coatings using magnetron sputtering in the metallic mode was previously shown in the example of the copper–oxygen system [8, 9]. A magnetron sputtering system equipped with a Cu target was used as a source of metal particle flux onto the substrate. The radio-frequency inductively coupled plasma (RF-ICP) source [10] was additionally used for dissociation and ionization of molecular oxygen in a vacuum chamber, which led to the growth of oxide coatings. However, copper is characterized by high sputtering yield and chemical affinity to react with oxygen, since the Gibbs energy (ΔG) of the growth of Cu_2O and CuO is −146 and −130 kJ/mol, respectively [11]. Both of these conditions lead to the possibility of magnetron deposition of oxide copper coatings in the metallic mode. Oppositely, yttrium has a low sputtering yield and higher Gibbs energy of the yttrium–oxygen system, which is equal to −1800 kJ/mol at 298 K [12]. Thus, it is necessary to estimate the possibility of deposition conditions of other coating materials, e.g. yttrium oxide.

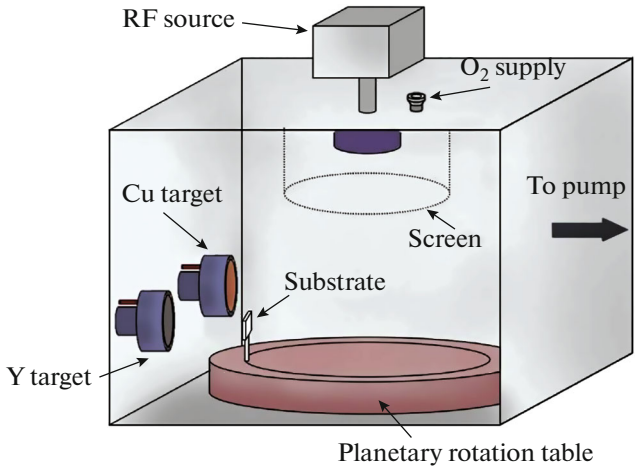

Fig. 1. Scheme of dual magnetron sputtering of yttrium–copper oxide coatings in the metallic mode.

This study is devoted to the collection of data on the regularities of the oxide coating deposition using magnetron sputtering in the metallic mode, enhanced by an RF-ICP source. Thus, the aim of this work was to determine the conditions for deposition of yttrium oxide coating using magnetron sputtering in the metallic mode.

MATERIALS AND METHODS

The experiments were carried out on a vacuum ion-plasma installation developed at the Weinberg Research Center of the Tomsk Polytechnic University, the scheme of which is shown in Fig. 1. The installation consists of a vacuum chamber equipped with a set of magnetron systems operating in the sputtering modes with single or dual targets, a planetary substrate holder, an RF-ICP source RPG-128 [10], and an pumping system based on a Shimadzu TMP-403LM turbomolecular pump (N_2: 420 L/s).

The experimental work was divided into two parts. The first one was devoted to determining the conditions for deposition of coatings of yttrium oxide by magnetron sputtering in the metallic mode. Four experiments were carried out using various sputtering process schemes, which are listed in Table 1. The sputtering schemes were as follows: single (no. 1) and dual Y-target sputtering (no. 2); single Y-target sputtering using the modified pumping system (no. 3) and dual sputtering of yttrium and copper targets (no. 4). In the case of the scheme no. 3, the pumping system was modified using an additional turbomolecular pump KYKY FF-160/700E (N_2: 700 L/s.). Other installation parameters were the same. The separation of argon and oxygen flows was used in all schemes: Ar was inflowed into the magnetron sputtering system with a Y-target, and oxygen was supplied near the RF-ICP source. The sputtering power densities for Y and Cu were 20.4 W/cm^2 for each target. The RF-ICP source power (13.56 MHz) and Ar flow rate were 1.25 kW and 30 sccm, respectively.

The second part of the experiments was aimed at studying the structure of oxide coatings obtained by dual magnetron sputtering in the metallic mode, enhanced by the RF-ICP source, according to scheme no. 4. The dual magnetron sputtering system was equipped with copper (90 mm in diameter and 6 mm thick, purity 99.9%) and yttrium targets (90 mm in diameter and 8 mm thick, purity 99.9%) with APEL-M-10DU power supply (Applied Electronics, Russia). The flow rate of O_2 was selected from the hysteresis loop (10 sccm). The deposition time was 30 min. Oxide films were deposited on polished AISI 321 stainless steel substrates (20 × 20 × 1 mm) and Si(110) wafers. Prior to deposition, the substrates were treated with isopropyl alcohol in an ultrasonic bath (20 min) and dried by compressed air. The substrates rotated planetary (5 rpm) during the deposition process. The thickness and elemental composition of oxide films were studied using a scanning electron microscope Vega 3 (Tescan, Czech Republic) equipped with an attachment for energy dispersive spectroscopy. The crystal structure of the samples was determined by X-ray diffraction (Shimadzu XRD-7000S diffractometer, Cu$K_{\alpha 1}$ radiation, 40 kV, 30 mA) in the 2θ range 10°–90° with a scanning step of 0.0143°. Diffractograms were identified using the ICDD-4+ database.

RESULTS AND DISCUSSION

The hysteresis loops of the discharge voltage for four series of experiments are shown in Fig. 2. In order to plot the hysteresis loops and confirm the metallic deposition mode, the discharge voltage was recorded with a gradual increase and decrease in the oxygen flow rate with a step of 2 sccm. It is clearly seen that the

Table 1. Schemes for deposition of oxide films

No.	Power supply	Turbomolecular pump type	Target	S_0, m^3/s
1	Unipolar	Shimadzu TMP-403LM	Yttrium	0.24
2	Bipolar	Shimadzu TMP-403LM	Yttrium and yttrium	>0.60
3	Unipolar	Shimadzu TMP-403LM and KYKY FF-160/700E	Yttrium	0.61
4	Bipolar	Shimadzu TMP-403LM	Yttrium and copper	>0.87

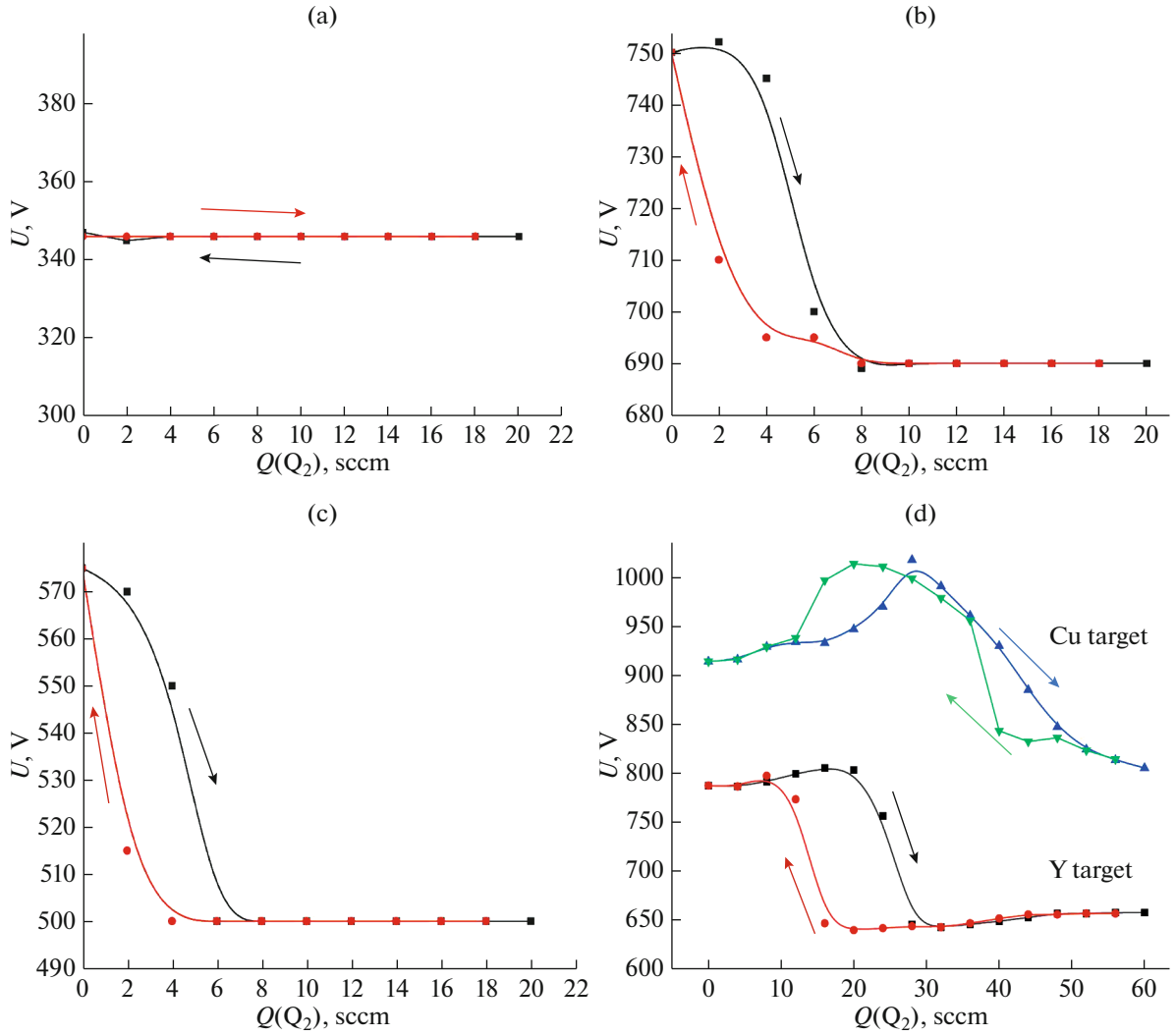

Fig. 2. Hysteresis loops of the discharge voltage at: (a) unipolar sputtering of a single yttrium target; (b) dual magnetron sputtering of two yttrium targets; (c) unipolar sputtering of a single yttrium target with an increased pumping speed; (d) dual magnetron sputtering of yttrium and copper targets.

hysteresis loop in the case of sputtering of a single yttrium target (scheme no. 1) corresponds only to the reactive deposition mode, which indicates the oxidation of the Y-target even at low oxygen flow rates (Fig. 2a). The absence of metallic and transition deposition modes is due two factors: the high Gibbs energy for the yttrium–oxygen system (–1800 kJ/mol at 298 K [12]) and the low sputtering yield of Y-target [13, 14]. Using the dual magnetron sputtering of two yttrium targets (Fig. 2b) leads to a shift in the hysteresis curve towards higher oxygen flow rates. A hysteresis section from zero to 8 sccm of O_2 flow rate is clearly visible, corresponding to the appearance of the transition deposition mode. A similar effect was found when scheme no. 3 was used with the increased pumping speed (Fig. 2c).

Figure 2d shows that the dual magnetron sputtering of Y- and Cu-targets (scheme no. 4) can be used to deposit oxide coatings in the metallic mode. The observed shift of the hysteresis loop in comparison with other schemes is due to several factors. First, the higher sputtering yield of copper compared to yttrium in the metal and oxide states results in a higher flux of metal particles from the Cu-target compared to the flux from the Y-target. Second, since the activation energy of the Cu–O system is negative (–173.2 kJ/mol [12]), Cu atoms can interact with oxygen ones, forming copper oxide coatings. Both of these factors lead to a decrease in the concentration of oxygen atoms near the yttrium target and its sputtering in the metallic mode [15]. Therefore, the speed of oxygen pumping from the sputtering zone plays a key role in the sputtering of an yttrium target in the Ar + O_2 atmosphere in

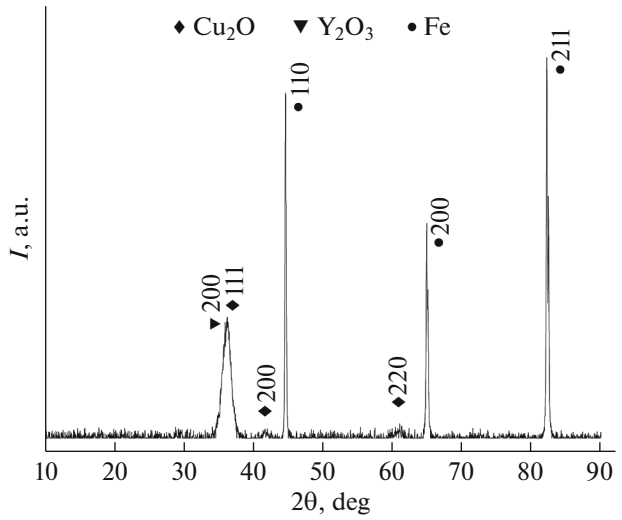

Fig. 3. X-ray diffraction pattern of an yttrium–copper oxide film deposited by dual magnetron sputtering in the metallic mode, enhanced by RF-ICP source.

the metallic mode. So, it is necessary to calculate and compare effective pumping speeds for all schemes of deposition of yttrium oxide coatings.

The effective pumping rates for schemes no. 1 and 3 were calculated from the basic equation of vacuum technology [16]:

$$1/S_0 - 1/S_p = 1/U,$$

where S_0 is the effective pumping speed [m^3/s], S_p is the pump rate [m^3/s], U is the conductivity of the pumping line [m^3/s].

The rate of the Shimadzu TMP-403LM turbomolecular pump is 0.42 m^3/s, the KYKY FF-160/700E pump is 0.7 m^3/s. The conductivity of the main pumping line is calculated using the following equation [16]:

$$1/U_\Sigma = 1/U_{INL} + 1/U_{ANG} + 1/U_G + 1/U_P,$$

where U_{INL} is the inlet conductivity, U_{ANG} is the conductivity of the angle pipe, U_G is the conductivity of the high-vacuum gate, and U_P is the conductivity of the pipe. The effective pumping speed for scheme no. 4 was calculated as follows [16]:

$$S_0 = \beta_0 V_0 A,$$

where V_0 is the volume of gas entering the getter surface (thin copper film) with an area (A) per 1 s at a certain temperature, β_0 is the adsorption coefficient for copper atoms. The volume of gas entering the getter surface can be calculated using the following equation:

$$V_0 = 36.38A(T/M)^{0.5},$$

where T is the temperature [K] and M is the molecular weight [a.m.u.]. In the calculations, the coefficient of adsorption of oxygen atoms by copper was assumed to be unity, the temperature was 293 K, and the surface area of the getter film was 80 cm^2 (the minimum area for deposition of copper oxide coatings). The results of calculating S_0 are presented in Table 1. The effective pumping speed for deposition scheme no. 2 could not be accurately determined.

Based on the calculations, the sputtering of an yttrium target in the Ar + O_2 atmosphere in the metallic mode was found to be possible at an effective pumping speed of more than 0.87 m^3/s. Since the sputtering of an yttrium target in the metallic mode can be carried out using scheme no. 4, the future coating deposition of an oxide film was studied for this case.

Figure 3 shows the X-ray diffraction pattern of the oxide coating obtained by dual magnetron sputtering in the metallic mode. Based on the ICDD-4+ database, the Cu_2O (JCPDS no. 78-2076) and Y_2O_3 (JCPDS no. 76-151) phases were identified. The α-Fe phase (JCPDS no. 65-4899) corresponds to the substrate material. The elemental composition of oxide film is presented in Table 2. The elements Cu (42.8 at %), Y (11.2 at %), and O (46.0 at %) were found, which corresponds to the Cu/Y ratio of 3.8. Using TRIM [17], the sputtering yields for Cu- and Y-targets by Ar ions were calculated, which are equal to 3.18 and 0.97 atom/ion and correlate well with the literature data [18]. The sputtering yields for oxidized targets of Cu- and Y-targets decrease approximately by factors of 2.5 and 30 [12, 19, 20], respectively. Table 3 shows the sputtering yields of copper and yttrium targets in the metallic and reactive (oxidized) modes. Comparison of the elemental composition of the deposited coatings with sputtering yields indicates the metallic state of both Cu and Y targets (scheme no. 4). The data obtained show the possibility of using magnetron sputtering of Y-target in the metallic mode for deposition of yttrium oxide coatings.

Table 2. Elemental composition (at %) of the sample

O	Cu	Y	Cu/Y ratio
46.0 ± 1.8	42.8 ± 1.6	11.2 ± 0.2	~3.8

Table 3. Calculated sputtering yield (atom/ion) of yttrium and copper targets

Deposition mode	Cu	Y
Metallic	1.5	0.5
Reactive	0.6	0.017

CONCLUSIONS

Magnetron sputtering of an yttrium target in an Ar and O_2 atmosphere, enhanced by an RF-ICP source has been investigated. Four different sputtering schemes have been studied to confirm the metallic

mode of yttrium oxide coating deposition. The increase in the effective pumping speed is shown to lead to a shift of the hysteresis loop to higher O_2 flow rates and enable the target sputtering using the transition and metallic modes. The oxide coating consisting of Cu_2O and Y_2O_3 phases has been obtained by dual magnetron sputtering of yttrium and copper targets in the metallic mode, enhanced by RF-ICP source. The calculated sputtering yields for Cu and Y in the metallic and reactive modes indicate the coating deposition in the metallic mode.

FUNDING

This work was supported by the Russian Science Foundation (grant no. 22-29-01173).

CONFLICTS OF INTEREST

The authors declare no conflicts of interest.

REFERENCES

1. J. Zhu, Y. Zhu, W. Shen, Y. Wang, J. Han, G. Tian, and B. Dai, Thin Solid Films **519**, 4894 (2011). https://doi.org/10.1016/j.tsf.2011.01.049
2. E. Courcot, F. Rebillat, F. Teyssandierm, and C. Louchet-Pouillerie, J. Eur. Ceram. Soc. **30**, 1911 (2010). https://doi.org/10.1016/j.jeurceramsoc.2010.02.012
3. P. Lei, J. Zhu, Y. Zhu, C. Jiangm, and X. Yin, Appl. Phys. A **108**, 621 (2012). https://doi.org/10.1007/s00339-012-6940-4
4. M. Goral, S. Kotowski, A. Nowotnik, M. Pytel, M. Drajewiczm, and J. Sieniawski, Surf. Coat. Technol. **237**, 5 (2013). https://doi.org/10.1016/j.surfcoat.2013.09.028
5. A. Pakseresht, F. Sharifianjazi, A. Esmaeilkhanian, L. Bazli, M. R. Nafchi, M. Bazlim, and K. Kirubaharan, Mater. Des. **222**, 111044 (2022). https://doi.org/10.1016/j.matdes.2022.111044
6. D. Depla and S. Mahieu, *Reactive Sputter Deposition*, 1st ed. (Springer, Berlin, 2008).
7. P. Lei, W. Leroy, B. Dai, J. Zhu, X. Chen, J. Hanm, and D. Depla, Surf. Coat. Technol. **276**, 39 (2015). https://doi.org/10.1016/j.surfcoat.2015.06.052
8. D. V. Sidelev, E. D. Voroninam, and V. A. Grudinin, Vacuum **207**, 111551 (2023). https://doi.org/10.1016/j.vacuum.2022.111551
9. D. V. Sidelev, E. D. Voroninam, and G. A. Bleykher, Vacuum **211**, 111956 (2023). https://doi.org/10.1016/j.vacuum.2023.111956
10. E. V. Berlin and V. J. Grigoryev, US Patent No. 9704691 (11 July 2017).
11. D. R. Lide and G. Baysinger, *Handbook of Chemistry and Physics*, 92nd ed. (CRC, Boca Raton, 2011).
12. J. E. Burke, *Progress in Ceramic Science* (Elsevier, Amsterdam, 2013).
13. K. Strijckmans, R. Schelfhout, and D. Depla, J. Appl. Phys. **124**, 241101 (2018). https://doi.org/10.1063/1.5042084
14. R. Schelfhout, K. Strijckmans, and D. Depla, Surf. Coat. Technol. **399**, 126097 (2020). https://doi.org/10.1016/j.surfcoat.2020.126097
15. R. Behrisch, *Sputtering by Particle Bombardment* (Springer, New York, 1981).
16. L. N. Rozanov, Meas. Sci. Technol. **13**, 1654 (2002). https://doi.org/10.1088/0957-0233/13/10/708
17. J. Ziegler, J. P. Biersack, and M. D. Ziegler, TRIM (the Transport of Ions in Matter). http://www.srim.org.
18. M. Saraiva, V. Georgieva, S. Mahieu, K. Van Aeken, A. Bogaerts, and D. Depla, J. Appl. Phys. **107**, 034902 (2010). https://doi.org/10.1063/1.3284949
19. K. Strijckmans, W. P. Leroy, R. De Gryse, and D. Depla, Surf. Coat. Technol. **206**, 3666 (2012). https://doi.org/10.1016/j.surfcoat.2012.03.019
20. Y. Mao, J. Engels, A. Houben, M. Rasinski, J. Steffens, A. Terra, and J. W. Coenen, Nucl. Mater. Energy **10**, 1 (2017). https://doi.org/10.1016/j.nme.2016.12.031